Nanobodies With In Vitro Neutralizing Activity Protect Mice Against H5N1 Influenza Virus Infection

Lorena Itatí Ibañez,[1,2] Marina De Filette,[1,2] Anna Hultberg,[4] Theo Verrips,[4] Nigel Temperton,[5,6] Robin A. Weiss,[5] Wesley Vandevelde,[3] Bert Schepens,[1,2] Peter Vanlandschoot,[3] and Xavier Saelens[1,2]

[1]Department for Molecular Biomedical Research, VIB, [2]Department of Biomedical Molecular Biology, Ghent University, [3]Ablynx NV, Ghent, Belgium; [4]Cellular Architecture and Dynamics, Department of Biology, University of Utrecht, Utrecht, The Netherlands; [5]MRC/UCL Centre for Medical Molecular Virology, Division of Infection and Immunity, University College London; and [6]Viral Pseudotype Unit, Medway School of Pharmacy, University of Kent, Chatham Maritime, United Kingdom

Influenza A virus infections impose a recurrent and global disease burden. Current antivirals against influenza are not always effective. We assessed the protective potential of monovalent and bivalent Nanobodies (Ablynx) against challenge with this virus. These Nanobodies were derived from llamas and target H5N1 hemagglutinin. Intranasal administration of Nanobodies effectively controlled homologous influenza A virus replication. Administration of Nanobodies before challenge strongly reduced H5N1 virus replication in the lungs and protected mice from morbidity and mortality after a lethal challenge with H5N1 virus. The bivalent Nanobody was at least 60-fold more effective than the monovalent Nanobody in controlling virus replication. In addition, Nanobody therapy after challenge strongly reduced viral replication and significantly delayed time to death. Epitope mapping revealed that the VHH Nanobody binds to antigenic site B in H5 hemagglutinin. Because Nanobodies are small, stable, and simple to produce, they are a promising, novel therapeutic agent against influenza.

Highly pathogenic avian influenza (HPAI) H5N1 viruses pose a pandemic threat. Transmission of these viruses from birds to humans occurs rarely, but when it does, it often results in severe pulmonary and systemic disease with a mortality rate of 60%. Despite the availability of medicines designed to interfere with influenza viral functions [1], clinicians have very limited evidence-based intervention options to successfully treat victims of these zoonotic infections with HPAI H5N1. Currently licensed anti-influenza drugs are small molecules that target the ion channel activity of matrix protein 2 (amantadine and rimantadine) or the viral neuraminidase (oseltamivir and zanamivir). These drugs are beneficial in cases of uncomplicated influenza caused by susceptible influenza virus strains [2]. However, infection with HPAI H5N1 virus is often characterized by a more serious clinical outcome than uncomplicated influenza. This difference in severity can be attributed to the higher replication rate of HPAI H5N1 viruses, their broader cellular tropism and, sometimes, systemic spread [3–5]. Effective treatment and control of rapidly replicating HPAI H5N1 viruses (eg, with oseltamivir) may therefore require higher doses to obtain and maintain sufficient systemic drug concentrations [6]. Inadequate dosing, combined with prolonged virus replication, increases the odds of developing resistant virus strains [7, 8].

Severe infection with HPAI H5N1 is associated with an aberrant host immune response, producing high

Received 24 August 2010; accepted 18 November 2010.

Potential conflicts of interest: W.V. and P.V. are employees of Ablynx NV, which provided the recombinant VHH antibody fragments.

Presented in part: 14th International Conference on Negative Strand Viruses, Bruges, Belgium, June 2010. Abstract number 307.

Reprints or correspondence: Xavier Saelens, PhD, Department for Molecular Biomedical Research, VIB, and Department of Biomedical Molecular Biology, Ghent University, Technologiepark 927, Ghent, Belgium (xavier.saelens@dmbr.vib-ugent.be) or Peter Vanlandschoot, PhD, Ablynx NV, Technology Park 21, 9052 Ghent, Belgium (Peter.Vanlandschoot@Ablynx.com).

The Journal of Infectious Diseases 2011;203:1063–72

1537-6613/2011/2038-0001$15.00
DOI: 10.1093/infdis/jiq168

levels of circulating proinflammatory cytokines and chemokines [9]. Such potentially life-threatening cytokine deregulation is presumably caused by the unusual cellular and tissue tropism of HPAI H5N1 viruses, their rapid replication and the intrinsically high cytopathic outcome [10]. A combination of antiviral drugs and immunomodulators could be used to manage infection with HPAI H5N1, but such an intervention is not without risks [11–13]. Therefore, there is a need for novel anti-influenza drugs to treat patients with severe disease resulting from infection with highly pathogenic influenza viruses, or severe influenza in general.

Human or animal-derived immune serum with high titers of immunoglobulins against a particular virus has been used successfully to prevent and treat viral infections. For example, during the Spanish flu outbreak, passive immunotherapy with human convalescent blood products was used to treat patients with influenza pneumonia, with some success [14, 15]. A report from 2007 describes the transfer of convalescent plasma from a survivor of H5N1 influenza to treat a hospitalized 31-year-old patient with the same infection who had not responded to oseltamivir treatment. The patient recovered completely [16]. Compared with human immunoglobulin products, recombinant monoclonal antibodies or antibody-derived fragments are safer, better characterized, and more reliable therapeutics [17, 18]. The antigen-binding site of conventional antibodies resides in the paired variable domains of the heavy and light immunoglobulin chains. Antigen specificity is usually retained in recombinant single-chain variable fragment molecules, which typically comprise the variable heavy and variable light chain fragments from natural antibodies, linked by a flexible peptide [19], but antibodies with still smaller antigen-binding domains also exist naturally. Camelids and sharks produce immunoglobulins composed only of heavy chains, and the antigen-binding site of these antibodies resides in a single protein domain, designated VHH (or Nanobody [Ablynx]) in camelids [20, 21]. VHHs can be selected by phage or other display technologies, they are easily produced in robust recombinant expression systems, and they have high solubility and thermal stability. In addition, they can form long, fingerlike loops that can penetrate into the cavities of immunogens, and their small size permits good tissue penetration in vivo [22]. These characteristics have spurred the development of VHH-based proteins as novel therapeutic and diagnostic tools directed against multiple targets, including cytokines, enzymes, bacterial toxins, tumor antigens, microbial antigens, and parasites [23–28].

Here, we describe a novel treatment strategy for H5N1 influenza virus infection, based on recombinant neutralizing Nanobodies directed against hemagglutinin (HA). We show that intranasal administration of a Nanobody specific for H5N1-HA potently suppresses replication of a recombinant H5N1 virus in vivo. We also demonstrate that a bivalent H5N1-HA–specific Nanobody is at least 60-fold more effective at suppressing virus replication than its monovalent counterpart, as deduced from an in vivo dose-response comparison, and that it protects against a lethal H5N1 virus challenge. Analysis of selected escape mutant viruses allowed us to map the epitope of the protective Nanobody at the site corresponding to the antigenic site B in the HA molecule.

MATERIALS AND METHODS

Selection, Expression and Purification of H5 HA–Specific VHH Nanobodies

The recombinant H5N1-HA–specific VHHs (H5-VHH) Nanobodies used in this study have been described elsewhere (Anna Hultberg, Nigel J. Temperton, Valérie Rosseels, Mireille Koenders, Maria Gonzalez-Pajuelo, Bert Schepens, Lorena Itatí Ibañez, Peter Vanlandschoot, Joris Schillemans, Michael Saunders, Robin A. Weiss, Xavier Saelens, José A. Melero, C. Theo Verrips, Steven Van Gucht, and Hans J. De Haard, unpublished report). In brief, 2 llamas were immunized with recombinant clade 1 A/Vietnam/1203/2004 H5N1-HA (Protein Sciences) in Specol adjuvant. After 6 immunizations, total RNA was extracted from peripheral blood lymphocytes, converted into complementary DNA (cDNA), and cloned in a phagemid vector to generate a VHH phage display library. Phages carrying H5N1-HA–specific Nanobodies were selected by panning on immobilized H5N1-HA. The VHH-coding sequences from enriched phages were cloned into an *Escherichia coli* expression vector and purified from the bacterial periplasmic fraction by immobilized metal-affinity chromatography. Recombinant H5-VHHm Nanobody was used in this study. H5-VHHm Nanobody was also engineered into bivalent H5-VHHb, by linking 2 H5-VHHm domains with a glycine-serine linker. For a negative control VHH, we used recombinant monovalent respiratory syncytial virus (RSV) RSV-VHHm or bivalent RSV-VHHb (Hultberg et al, unpublished report). The endotoxin content of the purified, recombinant VHH antibodies was <1 EU/μg of protein, as determined with the limulus amebocyte lysate test.

H5N1 Influenza Virus

H5N1 influenza A virus NIBRG-14 was obtained from the UK National Institute for Biological Standards and Control, a center of the Health Protection Agency. NIBRG-14 is a 2:6 reverse genetics–derived reassortant of A/Vietnam/1194/2004 (H5N1) and A/PR/8/34 (H1N1) viruses. The HA- and neuraminidase-coding segments of NIBRG-14 are from A/Vietnam/1194/2004, but the HA segment lacks the polybasic cleavage site. NIBRG-14 virus was passaged 7 times in specific-pathogen–free BALB/c mice to obtain a mouse-adapted derivative (NIBRG-14ma) and propagated in Madin-Darby canine kidney (MDCK) cells. The HA-coding region was sequenced and found to be identical in NIBRG-14 and NIBRG-14ma viruses. The median tissue culture infectious dose ($TCID_{50}$) and median lethal dose (LD_{50}) of NIBRG-14ma virus were determined using the method of

Reed and Muench [29]; 1 LD_{50} of mouse-adapted NIBRG-14 corresponds to ~50 $TCID_{50}$. All experiments with NIBRG-14 and NIBRG-14ma viruses were performed in biosafety level 2 rooms with negative pressure relative to adjoining rooms.

Binding of Nanobodies to H5 HA

The affinity and avidity of myc-tagged H5-VHHm and VHHb were compared by performing an enzyme-linked immunosorbent assay on NIBRG-14ma–infected MDCK cells and on immobilized virions. MDCK cells were infected with 100 $TCID_{50}$ of NIBRG-14ma, and 8 h later cells were fixed with 4% paraformaldehyde. Binding of Nanobodies was revealed with an anti-myc monoclonal (Invitrogen) followed by horseradish peroxidase–labeled anti-mouse antibody (GE Healthcare) and horseradish peroxidase substrate (BD optEIA).

Prophylactic and Therapeutic Efficacy Studies in Mice

All animal procedures were approved by the Institutional Ethics Committee on Experimental Animals. Specific-pathogen–free female BALB/c mice, 7–9 weeks old, were purchased from Charles River (Germany) and used for all experiments. Mice were housed in cages individually ventilated with high-efficiency particulate air filters in temperature-controlled, air-conditioned facilities with food and water ad libitum. Mice were anesthetized by intraperitoneal injection of xylazine (10 μg/g) and ketamine (100 μg/g) before intranasal administration of Nanobodies or challenge virus (50 μL, divided equally between the nostrils). Nanobodies were diluted in endotoxin-free phosphate-buffered saline (PBS) with 1% (wt/vol) bovine serum albumin and administered as a single dose, ranging from 100 to 0.5 μg per mouse (5–0.25 mg/kg). Depending on the experiment, Nanobodies were administered up to 72 h before or after challenge, as specified in the figure legends.

To determine the effect of intranasal Nanobody delivery on lung virus titer production, mice were challenged with 1 LD_{50} of NIBRG-14ma virus and killed 4 days after challenge. Lung homogenates were prepared in PBS, cleared by centrifugation at 4°C, and used for virus titration. Monolayers of MDCK cells were infected with 50 μL of serial 1:10 dilutions of the lung homogenates, in a 96-well plate in serum-free Dulbecco's modified Eagle medium (Invitrogen) supplemented with penicillin and streptomycin. After 1 h, the inoculum was replaced by medium containing 2 μg/ml of L-(tosylamido-2-phenyl) ethyl chloromethyl ketone–treated trypsin (Sigma). End-point virus titers were determined by hemagglutination of chicken red blood cells and expressed as $TCID_{50}$ per milliliter. Influenza RNA levels were determined with quantitative polymerase chain reaction (PCR). RNA was isolated from 150 μL of cleared lung homogenate using the Nucleospin RNA virus kit (Machery-Nagel). The relative amount of NIBRG-14ma genomic RNA was determined by preparing viral cDNA and performing quantitative PCR with M-genomic segment primers 5'tcgaaaggaacagcagagtg3' and 5'ccagctctatgctgacaaaatg3' and probe 5'ggatgctg3' (probe no. 89; Universal ProbeLibrary, Roche) and the LightCycler 480 Real-Time PCR System (Roche).

To determine the degree of protection against mortality, mice were challenged with 4 LD_{50} of NIBRG-14ma virus and subsequently monitored for 14 days. A 25% loss in body weight was the end point at which moribund mice were euthanized.

Selection and Characterization of H5N1-HA–Specific VHH Escape Mutant Viruses

In vitro NIBRG-14ma escape viruses were isolated independently by selection with H5-VHHm and H5-VHHb Nanobodies. Virus was serially diluted and used to infect MDCK cells in the presence of H5-VHHm (5 μmol/L, corresponding to 500-fold the median inhibitory concentration in microneutralization) or H5-VHHb (0.05 μmol/L, corresponding to 5000-fold the median inhibitory concentration in microneutralization). Escape viruses were selected using standard techniques. After 10 passages in the presence of Nanobodies, escape viruses were plaque purified by growth on MDCK cells overlaid with 0.6% low-melting agarose in the presence of Nanobodies. Six escape virus isolates obtained by selection with H5-VHHm and 6 by selection with H5-VHHb were amplified on MDCK cells, still in the presence of the respective Nanobodies. Total RNA was extracted from the supernatant and used to clone the cDNA corresponding to the HA and M viral RNA (vRNA) segments, as described elsewhere [30]. In parallel, HA- and M-vRNA segments from the parental NIBRG-14ma were also cloned. Deduced amino acid substitutions in the HA sequence of escape viruses were modeled with PyMOL Molecular Graphics System (W. L. DeLano, 2002; DeLano Scientific) using the H5 HA structure with PDB code 2IBX [31]. Hemagglutination inhibition, receptor-binding experiments (using chicken and human erythrocytes, respectively), and microneutralization were performed as described elsewhere [32].

Statistical Analysis

SigmaPlot software (version 11) was used for statistical analysis. Differences between groups were tested using the Kruskal-Wallis 1-way analysis of variance on ranks. When this test demonstrated a significant difference between groups ($P < .05$), 2 correcting methods for multiple comparisons were used (Dunn's and Tukey's tests); t tests were used to compare 2 groups. Kaplan-Meier survival curves were plotted and evaluated.

RESULTS

Prophylactic Therapy with H5N1-HA–Specific Nanobodies

Nanobodies with clade 1 and clade 2 H5N1 virus neutralization activity have been described elsewhere (Hultberg et al, unpublished report). Bivalent H5-VHHb had a higher affinity and avidity for viral HA than its monovalent counterpart

H5-VHHm, in particular when binding to immobilized virions (Figure 1). We extended these finding using a mouse model for H5N1 challenge. Mice were administered PBS or 100 μg (5 mg/kg) of H5-VHHb or negative control RSV-VHHb intranasally at 4, 24 or 48 h before infection with 1 LD_{50} of NIBRG-14ma virus. Weight loss was monitored daily, and on day 4 mice were killed to determine virus replication in the lungs. All mice that received H5-VHHb retained their original body weight, whereas those receiving PBS or RSV-VHHb gradually lost weight (Figure 2*A*). Importantly, intranasal administration of H5-VHHb at 4 or 24 h before challenge did not result in detectable lung virus titers. When animals were treated with H5-VHHb 48 h before challenge, virus titers were 50-fold lower than in PBS and RSV-VHHb treated mice, and 3 of 7 animals had no detectable virus titers (Figure 2*B*).

In vitro, H5-VHHb had a 1000-fold higher virus neutralizing activity than H5-VHHm. We therefore compared the protective efficacy of monovalent H5-VHHm and bivalent H5-VHHb by administering different doses of the bivalent Nanobody, ranging from 60 to 0.5 μg per mouse (3 to 0.025 mg/kg) and equimolar amounts of the monovalent Nanobody (30 to 0.25 μg per mouse, corresponding to 1.5 to 0.012 mg/kg), 4 h before challenge. For up to 4 days after challenge, none of the mice treated with mono- or bivalent H5-specific VHH Nanobodies lost weight, but control VHH-treated mice lost up to 15% of their initial body weight (Figure 3*A*). Mice treated with PBS or with control VHH had lung virus titers ranging from 5×10^7 to 1×10^9 $TCID_{50}$/mL, whereas the virus titers in lung extracts from animals that received the highest dose of mono- or bivalent H5-VHH were below the detection limit (Figure 3*B*).

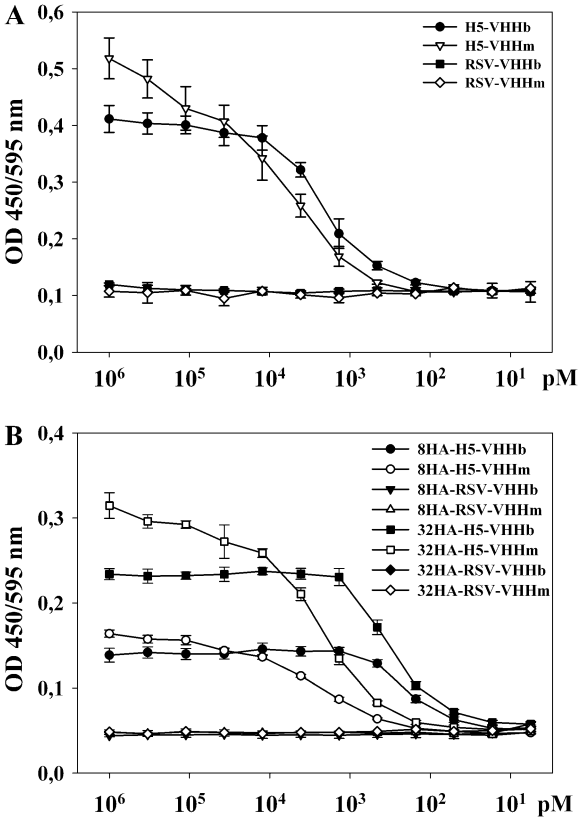

Figure 1. Binding of mono- and bivalent Nanobodies to H5N1 virus hemagglutinin (HA). *A,* Madin-Darby canine kidney cells were infected with 100-fold the median tissue culture infectious dose of NIBRG-14ma; 8 h later, binding of monovalent H5-VHHm and bivalent H5-VHHb, applied as 3-fold dilutions, was revealed by enzyme-linked immunosorbent assay (ELISA). Nanobodies specific for respiratory syncytial virus protein F (RSV-VHH) were used as negative controls. *B,* ELISA plates were coated with NIBRG-14ma virus (8 or 32 HA units, as indicated) to compare binding of mono- and bivalent Nanobodies (applied as 3-fold dilutions) by ELISA. Error bars represent standard deviations of the mean, calculated from 2 independent experiments performed in triplicate.

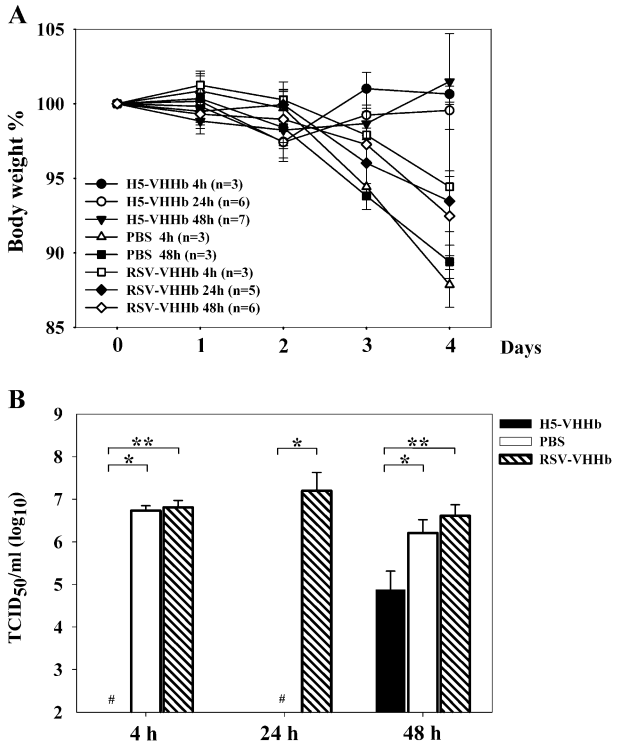

Figure 2. H5-VHHb inhibits replication of H5N1 virus in mice. *A,* Groups of 6–8-week-old BALB/c mice were given 100 μg of bivalent H5-VHHb, irrelevant control respiratory syncytial virus (RSV) VHHb or phosphate-buffered saline (PBS) intranasally at different time points before challenge with the median lethal dose of NIBRG-14ma virus. Subsequently, body weight was measured daily and is represented as the percentage of initial body weight. When mice were treated 4 or 48 h before infection, differences in body weight between the H5-VHHb and PBS groups were statistically significant ($P < .01$; analysis of variance). When mice were treated 24 h before infection, the differences between mice treated with H5-VHHb and both the PBS and RSV-VHHb groups were statistically significant ($P < .05$; *t* test). *B,* All mice were treated as described for *A* and killed on day 4 after challenge, and lung virus titers were determined. Graphs represent mean virus titers (median tissue culture infectious dose [$TCID_{50}$]/mL lung homogenate) for all mice in each group; error bars, standard deviations of the mean; #, below detection limit. $^*P < .05$; $^{**}P < .005$.

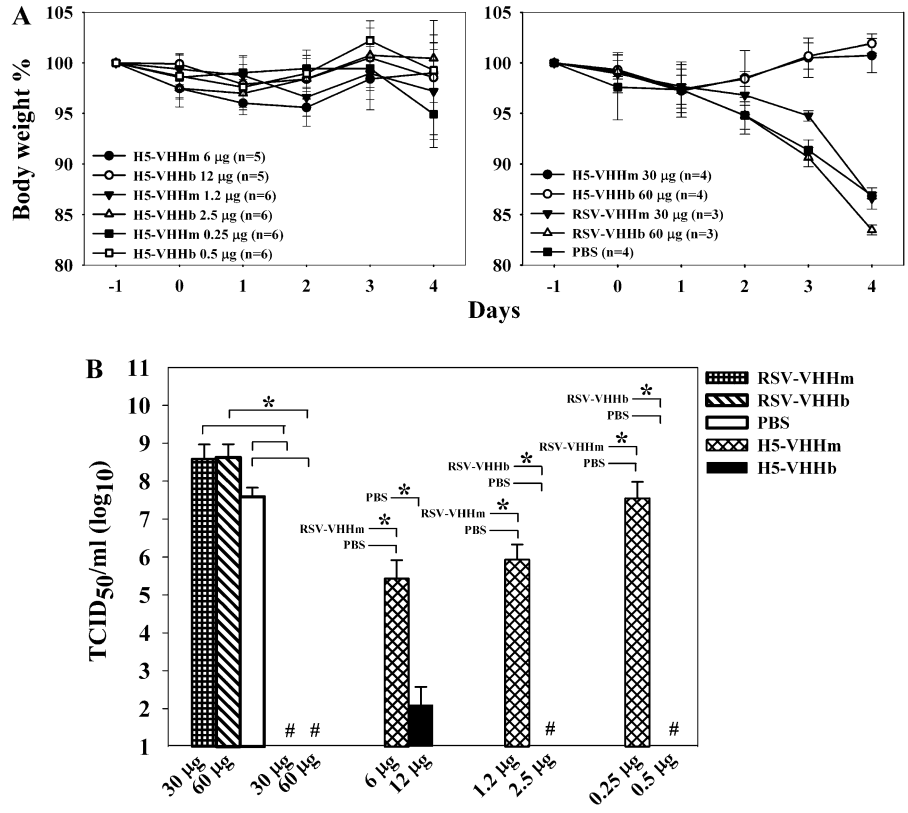

Figure 3. Bivalent H5-VHHb is more protective than monovalent H5-VHHm. *A,* BALB/c mice received phosphate-buffered saline (PBS), H5-VHHm, or H5-VHHb intranasally 24 h before challenge with the median lethal dose of NIBRG-14ma virus. Subsequently, body weight was measured daily and is represented as the average percentage of body weight for all mice in each group. The difference in weight loss was significant between mice given 30, 60, 6, 0.25 or 0.5 μg of H5-VHHm/b and those given respiratory syncytial virus (RSV) VHHm/b ($P < .01$). Similarly, the difference was significant at $P < .05$ between mice receiving 12 or 1.2 μg of H5-VHHm/b and those receiving RSV-VHHm/b, and at $P < .05$ between all doses of H5-VHHm/b and PBS. *B,* All mice were treated as described for *A* and killed on day 4 after infection, and lung virus titers were determined. Graphs represent mean virus titers (median tissue culture infectious dose [$TCID_{50}$]/mL lung homogenate) for all mice in each group; error bars, standard deviations of the mean; #, below detection limit. $*P < .05$.

Remarkably, prophylactic treatment with as little as 0.5 μg of H5-VHHb resulted in lung virus titers that were below the detection limit. It should be noted that we detected a low titer of virus in 1 of 4 mice treated with 12 μg of H5-VHHb Nanobody. Although the monovalent H5-VHHm was a less potent inhibitor of virus replication, treatment of mice with 6 or 1.2 μg of this molecule still resulted in significantly lower virus titers than in controls (Figure 3*B*).

Finally, we determined the protective efficacy of H5-VHHb over a longer period and with a higher challenge dose. As shown in Figure 4, mice that received 60 μg of H5-VHHb Nanobody 24 h before challenge with 4 LD_{50} of NIBRG-14ma were completely protected and displayed no weight loss, whereas all control mice had died or were moribund and had to be euthanized by day 8 after challenge.

Therapeutic Efficacy of H5N1-HA–Specific Nanobodies

We next determined whether H5-VHHb Nanobody could be used therapeutically. We administered 60 μg of this Nanobody (3 mg/kg) intranasally to mice up to 72 h after challenge with 1 LD_{50} of NIBRG-14ma virus. At 4 days after challenge, animals that had received H5-VHHb 4, 24 or 48 h after challenge had significantly higher body weights and lower lung virus loads than control mice (Figure 5). Although mice treated with H5-VHHb Nanobody 72 h after challenge were not clinically protected compared with control mice, they had significantly lower lung virus titers (Figure 5*B*). To exclude possible interference of residual neutralizing Nanobodies in the $TCID_{50}$ assay that was used to determine the viral loads in lung virus extracts, the amount of viral RNA in these extracts was also determined using vRNA-specific quantitative reverse-transcription PCR. The results of this assay were completely in line with the determined infectious virus load (Figure 5*C*). Because H5-VHHb Nanobody showed the strongest prophylactic activity, its therapeutic efficacy against a more lethal virus dose was determined. When 60 μg (3 mg/kg) of this VHH was given 48 or 72 h after infection with 4 LD_{50} of NIBRG-14ma, weight loss was lower than in controls. In addition, treatment with nanobodies 48 h after infection significantly delayed mortality compared with controls (Figure 6).

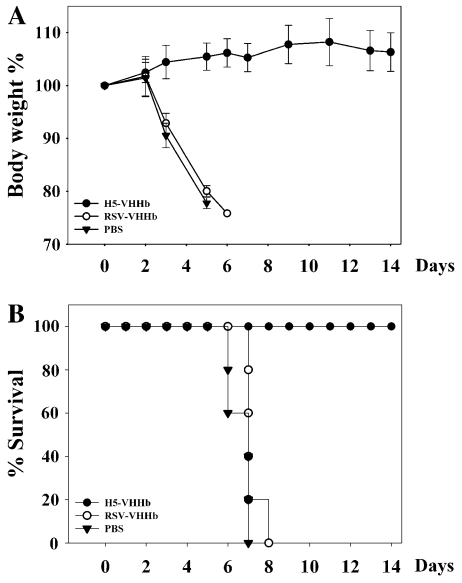

Figure 4. H5-VHHb protects against morbidity and mortality after H5N1 virus challenge. BALB/c mice ($n = 5$ per group) were given phosphate-buffered saline (PBS), 60 μg of respiratory syncytial virus (RSV) VHHb, or 60 μg of H5-VHHb intranasally; 24 h later (day 0) they were challenged with 4-fold the median lethal dose of NIBRG-14ma virus. Body weight and survival were monitored daily for 14 days. *A,* Body weight after infection is represented as the mean percentage of initial body weight for all mice in each group. Error bars represent standard deviations of the mean. There were significant differences in body weight between mice treated with H5-VHHb and both PBS and RSV-VHHb groups ($P < .01$) on day 5 after challenge. *B,* Kaplan-Meier survival curve of experiment in *A*.

Generation of H5-VHH Escape Variant H5N1 Virus

To identify the HA amino acid residues involved in H5-VHH binding, we selected escape viruses by growth and plaque purification of NIBRG-14ma virus in the presence of H5-VHHm or H5-VHHb Nanobodies. The HA sequences of 6 independently isolated H5-VHHm escape viruses revealed substitution of a lysine by a glutamic acid residue at position 189 in HA1 (H5 numbering). In addition, 2 H5-VHHm escape mutants carried an N154D substitution, and 4 carried an N154S substitution. The 3-dimensional structure of NIBRG-14 HA shows that N154D/S and K189E are close to each other as part of the corresponding antigenic site B in H3 HA (Figure 7*A*) [31, 33]. Interestingly, the N154D/S mutations remove an N-glycosylation site, which presumably has evolved in H5N1 HA as a strategy to mask an antigenic site [34]. Escape viruses selected in the presence of H5-VHHb carried only substitution K189N ($n = 4$) or K189E ($n = 2$). Notably, 4 of the H5-VHHb escape viruses had an additional D145N mutation located in the stalk of HA2, 40 residues upstream of the membrane anchor (Figure 7*B*). Based on hemagglutination inhibition and microneutralization assays, the K189N/E substitution appears necessary and sufficient to abolish binding to H5-VHHm or VHHb

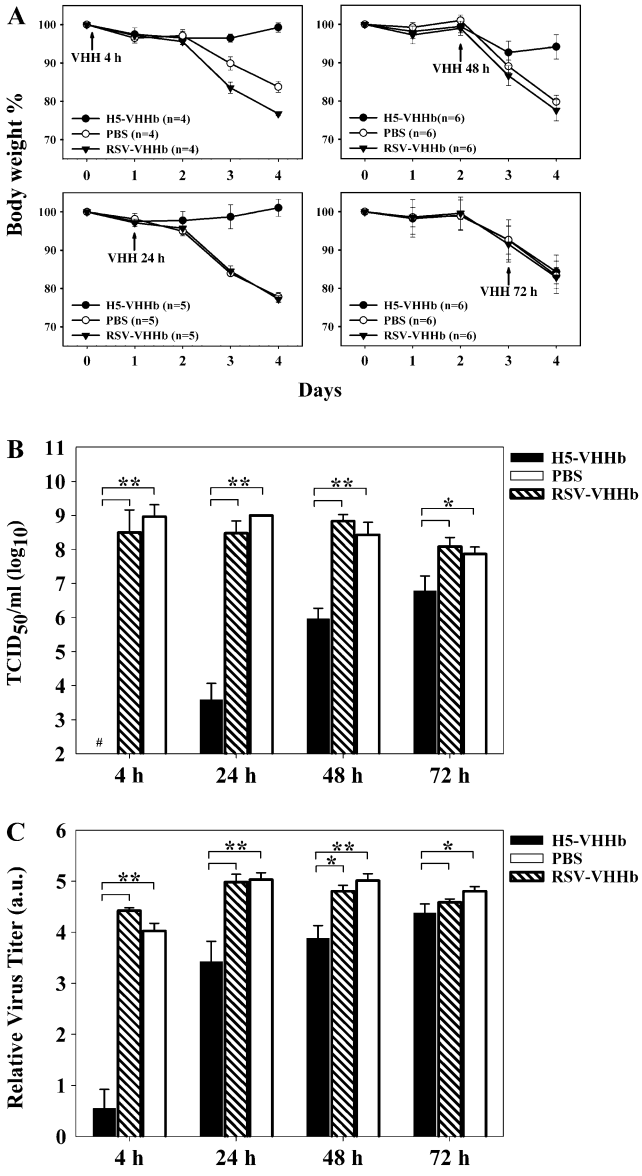

Figure 5. H5-VHHb inhibits H5N1 virus replication when administered up to 72 h after challenge. BALB/c mice were challenged with the median lethal dose of NIBRG-14ma virus. At 4, 24, 48, and 72 h after challenge, mice were treated intranasally with phosphate-buffered saline (PBS), 60 μg of control respiratory syncytial virus (RSV) VHHb, or 60 μg of H5-VHHb. *A,* Body weight after infection is represented as the mean percentage of initial body weight for all mice in each group. Four days after infection, there were significant differences in body weight ($P < .05$) between groups treated 4, 24, or 48 h after infection with H5-VHHb, RSV-VHHb, or PBS. *B,* Lung virus titers on day 4 after infection are represented as average virus titers (median tissue culture infectious dose [$TCID_{50}$]/mL lung homogenate) for all mice in each group. Statistically significant differences between compared groups (indicated with brackets) were obtained with $^{*}P < .05$ or $^{**}P < .005$. *C,* Viral genomic RNA load in lung extracts sampled on day 4 after infection as determined by quantitative reverse-transcription polymerase chain reaction and expressed as arbitrary units (a.u.). Error bars represent standard deviations of the mean.

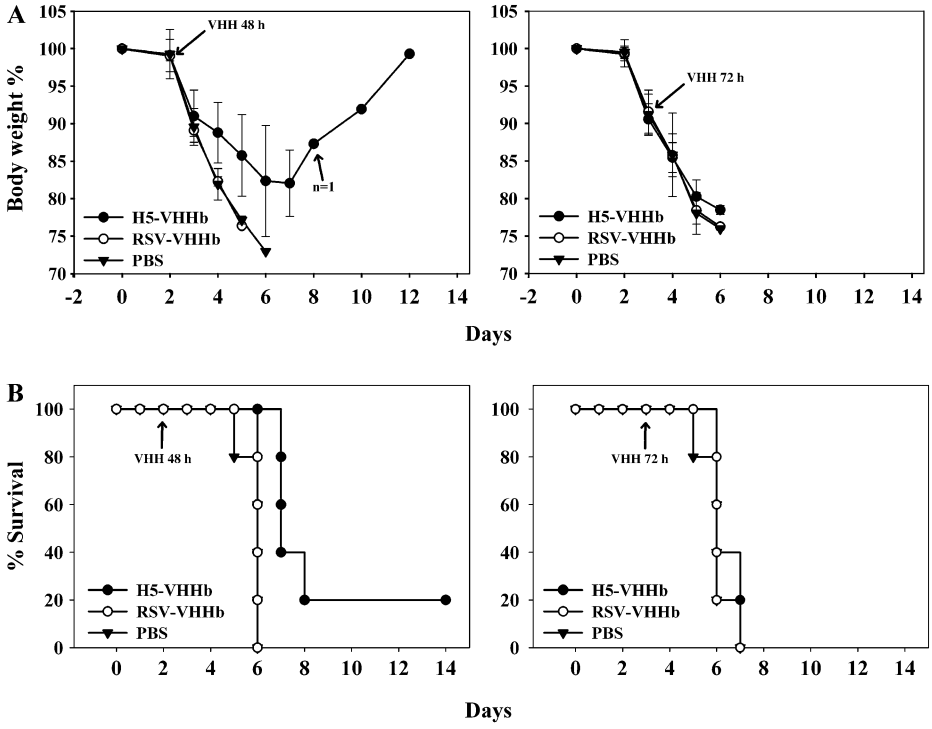

Figure 6. Therapeutic effect of H5-VHHb against severe H5N1 virus challenge. BALB/c mice ($n = 5$ per group) were challenged with 4-fold the median lethal dose of NIBRG-14ma virus. At 48 or 72 h after challenge, mice were treated intranasally with phosphate-buffered saline (PBS), 60 μg of respiratory syncytial virus (RSV) VHHb, or 60 μg of H5-VHHb. *A,* Body weight after infection is represented as the average percentage of body weight for all mice in each group. Error bars represent standard deviations of the mean. Differences were significant on day 5 after challenge between mice treated with H5-VHHb 48 h after infection and those treated with PBS or RSV-VHHb ($P < .01$). *B,* Kaplan-Meier survival curve for experiment in *A*. The difference in survival rate is significant ($P < .01$) between control mice (treated with PBS or RSV-VHHb) and mice treated with H5-VHHb 48 h after infection.

(Figure 7*C* and *D*). These results indicate that residues in antigenic site B, at the top of HA and very close to the receptor binding domain, are essential for neutralization by H5-VHHm/b.

DISCUSSION

Despite decades of research on antivirals to treat influenza, there are still very few virus-directed options for the treatment of patients with severe complications of influenza. Zoonotic infections with H5N1 influenza viruses are rare, but the case-fatality rate is ~60% even when advanced supportive therapy is applied [35]. We demonstrated that intranasal administration of llama-derived immunoglobulin single-chain variable domain fragments with in vitro neutralizing activity against H5N1 viruses can control virus replication and reduce morbidity and mortality in a mouse model for H5N1 influenza. We also showed that the in vivo neutralizing capacity of bivalent H5 HA–specific Nanobodies is superior to that of the monovalent construct. Indeed, when mice were treated with as little as 25 μg/kg of H5-VHHb 24 h before challenge, virus titers in the lungs were undetectable. Compared with treatment with an irrelevant Nanobody, significant reductions in lung virus loads were obtained by prophylactic administration of H5-VHHb up to 2 days before challenge or by therapeutic treatment for up to 3 days after challenge.

Different groups of investigators have reported the isolation and characterization of murine or human monoclonal antibodies and single-chain variable fragment antibody fragments that are reactive against H5 HA with specificity for a particular clade of H5 HA [36], cross-clade reactivity [37–40], and even reactive against multiple HA subtypes [41–44]. How do our findings compare with these and findings of other studies that have explored passive immunoprophylaxis as a promising therapeutic against influenza? First, Nanobodies can be easily produced in and purified from a prokaryotic or yeast expression system. Second, Nanobodies can be engineered into multiple configurations to produce, for example, bispecific, bivalent, or pentavalent constructs [45]. Third, we chose the intranasal or intrapulmonary route of administration because this allows deposition and deep penetration of Nanobodies in the respiratory tract. Fourth, H5-VHHb at 25 μg/kg was able to control lung virus replication when administered 24 h before challenge. In most other studies, passive immunotherapy was applied at doses between 3 and 25 mg/kg. However, the

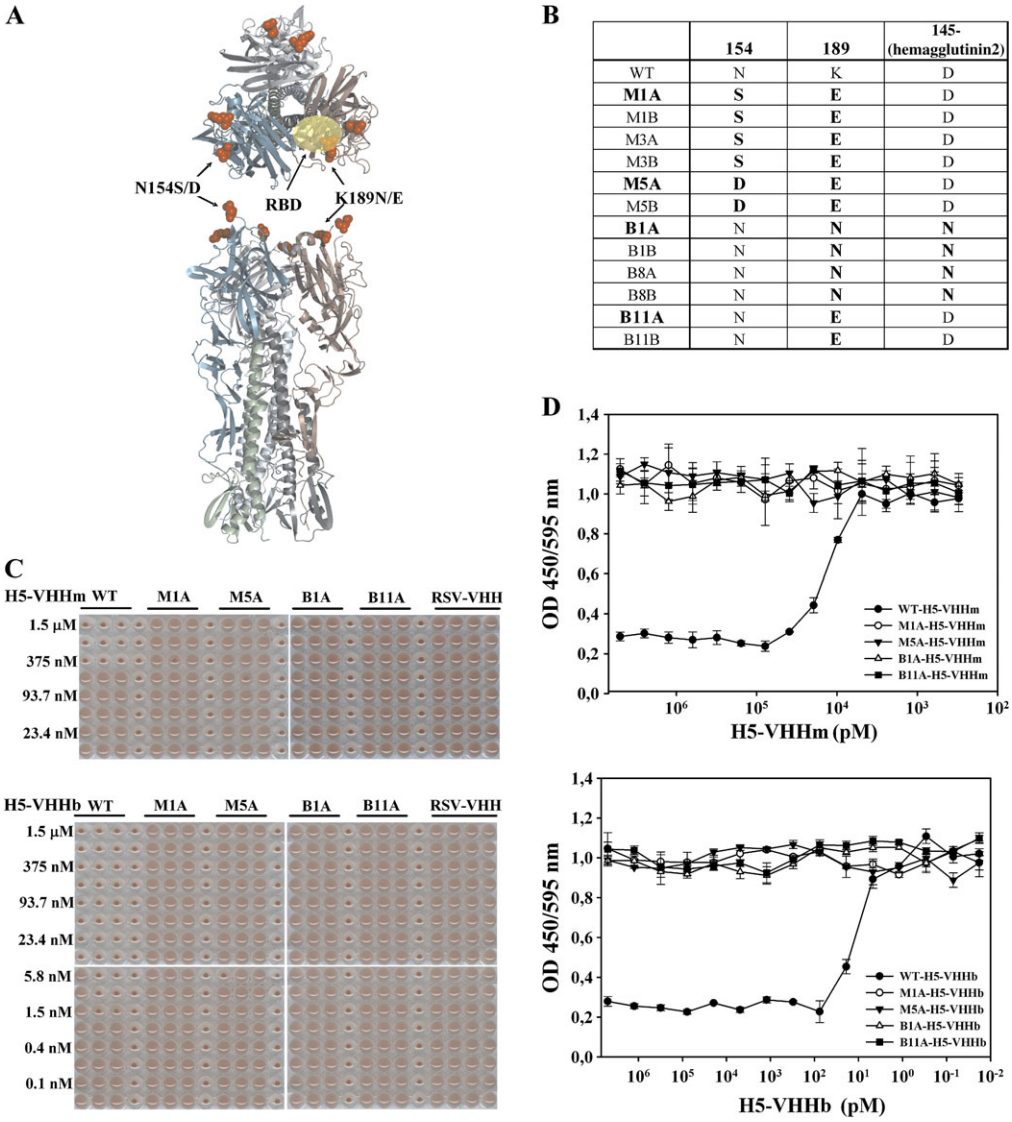

	154	189	145- (hemagglutinin2)
WT	N	K	D
M1A	**S**	**E**	D
M1B	**S**	**E**	D
M3A	**S**	**E**	D
M3B	**S**	**E**	D
M5A	**D**	**E**	D
M5B	**D**	**E**	D
B1A	N	**N**	**N**
B1B	N	**N**	**N**
B8A	N	**N**	**N**
B8B	N	**N**	**N**
B11A	N	**E**	D
B11B	N	**E**	D

Figure 7. Isolation and characterization of in vitro VHH escape viruses. *A,* Schematic representation of the likely antigenic site recognized by H5-VHH Nanobodies. NIBRG-14 hemagglutinin is represented as a ribbon in top and side views. Side chains of N154 and K189 (hemagglutinin 1 subunit and H5 numbering) that are substituted in H5-VHHm/b escape viruses are shown in red. The receptor binding domain (RBD) is highlighted in one monomer (*top view*). The image was generated using the PyMOL Molecular Graphics System (W. L. DeLano, 2002; DeLano Scientific) and Protein Data Bank accession number 2IBX. *B,* Overview of amino acid substitutions in hemagglutinin of escape viruses obtained after growth of NIBRG-14ma virus on Madin-Darby canine kidney cells in the presence of H5-VHHm (M) or H5-VHHb (B) Nanobodies. *C, D,* Wild-type NIBRG-14ma and escape virus isolates (highlighted in bold in *B*) were used in hemagglutination inhibition (*C*) and microneutralization (*D*) assays; 4 hemagglutinin units of each virus were used to agglutinate chicken erythrocytes in the presence of a 2-fold serial dilution of H5-VHHm (*top*) or H5-VHHb (*bottom*), and 100-fold the median tissue culture infectious dose of NIBRG-14ma was used in the microneutralization assay. Eighteen hours after infection the amount influenza virus nucleoprotein was determined by enzyme-linked immunosorbent assay of fixed cells.

comparison of doses has to take into account the 10-fold lower molecular mass of VHH molecules compared with conventional antibodies. Monovalent Nanobodies are small (~15 kDa) and as a result are removed rapidly from the blood through the kidneys. Their serum half-life is 30–60 min [46]. Half-life extension methods used for other small antibody fragments, such as PEGylation or fusion to serum albumin, could be used to tailor the half-life of Nanobodies.

Conventional immunoglobulins are normally multivalent, meaning that they have multiple paratopes for antigen binding. Nevertheless, such immunoglobulins, including neutralizing antibodies, mostly bind to a single virion with only one paratope [47]. The distribution of the viral spikes and their accessibility for antibody binding usually does not permit bivalent binding of a conventional antibody to a single virion. In addition, the flexibility of the 2 epitope-binding arms of an immunoglobulin

G molecule is limited, and therefore binding to a second epitope on the surface of a single virion is possible only when that epitope is very near. This paradigm of typically monovalent interaction between a neutralizing monoclonal immunoglobulin G and a viral spike protein has been elegantly addressed by Wang and Yang [48]. Neutralization of human immunodeficiency virus type 1 (HIV-1) by monoclonal antibody 2F5 was 100-fold enhanced when a second epitope for 2F5 was artificially introduced at another position in the HIV-1 glycoprotein spike, allowing bivalent interaction with increased binding avidity between the antibody and the virion. It was also demonstrated that such a bivalent binding occurs in trans, that is, by bridging the natural and artificially introduced epitopes in 2 subunits within a single HIV-1 trimer [48]. A similar mechanism may explain the superior neutralization and protective efficacy of bivalent H5-VHHb compared with H5-VHHm. The flexible linker between the 2 paratope-containing domains in H5-VHHb and its small size are compatible with a high-affinity bivalent interaction with 2 epitopes within a single HA trimer.

A K189E substitution in HA1 was found to abolish the neutralizing effect of H5-VHH. A Lys or Arg residue at this position is conserved in all human H5N1 virus isolates. Of note, all selected escape mutants contained a glutamic acid or serine residue at position 189, which indicates that the conserved positively charged amino acid is essential for H5-VHH binding. Interestingly, escape mutants selected with H5-VHHm also carried an N154D/S commutation that removes an N-glycosylation site in this antigenic site of HA. The predicted N-glycosylation site at N154 in A/Hong Kong/156/97 HA was shown to be glycosylated [49]. This N-glycosylation in H5 HA might have evolved to mask an antigenic site near the receptor binding domain [50]. It may facilitate H5-VHHm binding by increasing the thermodynamic stability of the epitope, contributing to a productive interaction with monovalent but not bivalent H5-VHH. Increased receptor affinity of HA [32] in selected H5-VHH escape viruses in vitro is less likely, because their susceptibility to receptor-destroying enzyme treatment is equal to that of the parental virus (results not shown).

We conclude that neutralizing Nanobodies have considerable potential for the treatment of H5N1 virus infections. Although we focused on VHHs that recognize an epitope near the receptor binding domain, it is possible to select VHH molecules that bind to other epitopes in HA, including more conserved domains.

Funding

Ablynx NV, Institute for the Promotion of Innovation by Science and Technology Flanders (grant IWT 70050 from the Flemish government), Belgian Federal Sciences Administration (Federale Wetenschapsbeleid, BELSPO) (grant to L.I.I.), Ghent University (IOF [Industrieel Onderzoeksfonds] Stepstone grant IOF08/STEP/001 to L.I.I.). B.S. is a postdoctoral fellow at FWO (Fonds voor Wetenschappelijk Onderzoek)-Vlaanderen.

Acknowledgments

We thank Dr Amin Bredan for editing the manuscript and Anouk Smet, Frederik Vervalle, and Tine Ysenbaert for excellent technical assistance. We are grateful to Dr John Wood from the UK National Institute for Biological Standards and Control for providing NIBRG-14 virus and to Dr Juerg Stech and Dr Olga Stech from FLI (Greifswald Insel-Riems) for providing a rapid influenza virus gene cloning system.

References

1. de Jong MD. H5N1 transmission and disease: observations from the frontlines. Pediatr Infect Dis J **2008**; 27:S54–6.
2. Nicholson KG. Aoki FY. Osterhaus AD. et al. Efficacy and safety of oseltamivir in treatment of acute influenza: a randomised controlled trial. Neuraminidase Inhibitor Flu Treatment Investigator Group. Lancet **2000**; 355:1845–50.
3. Gu J. Xie Z. Gao Z. et al. H5N1 infection of the respiratory tract and beyond: a molecular pathology study. Lancet **2007**; 370:1137–45.
4. Matrosovich MN. Matrosovich TY. Gray T. Roberts NA. Klenk HD. Human and avian influenza viruses target different cell types in cultures of human airway epithelium. Proc Natl Acad Sci U S A **2004**; 101:4620–4.
5. Rimmelzwaan GF. Nieuwkoop NJ. de Mutsert G. et al. Attachment of infectious influenza A viruses of various subtypes to live mammalian and avian cells as measured by flow cytometry. Virus Res **2007**; 129:175–81.
6. Govorkova EA. Ilyushina NA. Boltz DA. Douglas A. Yilmaz N. Webster RG. Efficacy of oseltamivir therapy in ferrets inoculated with different clades of H5N1 influenza virus. Antimicrob Agents Chemother **2007**; 51:1414–24.
7. de Jong MD. Tran TT. Truong HK. et al. Oseltamivir resistance during treatment of influenza A (H5N1) infection. N Engl J Med **2005**; 353:2667–72.
8. Gooskens J. Jonges M. Claas EC. Meijer A. Kroes AC. Prolonged influenza virus infection during lymphocytopenia and frequent detection of drug-resistant viruses. J Infect Dis **2009**; 199:1435–41.
9. de Jong MD. Simmons CP. Thanh TT. et al. Fatal outcome of human influenza A (H5N1) is associated with high viral load and hypercytokinemia. Nat Med **2006**; 12:1203–7.
10. Baskin CR. Bielefeldt-Ohmann H. Tumpey TM. et al. Early and sustained innate immune response defines pathology and death in nonhuman primates infected by highly pathogenic influenza virus. Proc Natl Acad Sci U S A **2009**; 106:3455–60.
11. Salomon R. Hoffmann E. Webster RG. Inhibition of the cytokine response does not protect against lethal H5N1 influenza infection. Proc Natl Acad Sci U S A **2007**; 104:12479–81.
12. White NJ. Webster RG. Govorkova EA. Uyeki TM. What is the optimal therapy for patients with H5N1 influenza? PLoS Med **2009**; 6:e1000091.
13. Zheng BJ. Chan KW. Lin YP. et al. Delayed antiviral plus immunomodulator treatment still reduces mortality in mice infected by high inoculum of influenza A/H5N1 virus. Proc Natl Acad Sci U S A **2008**; 105:8091–6.
14. Luke TC. Kilbane EM. Jackson JL. Hoffman SL. Meta-analysis: convalescent blood products for Spanish influenza pneumonia: a future H5N1 treatment? Ann Intern Med **2006**; 145:599–609.
15. Ross CW. Hund EJ. Treatment of the pneumonic disturbance complicating influenza, the transfusion of citrated immune blood. J Am Med Assoc **1919**; 72:640–45.
16. Zhou B. Zhong N. Guan Y. Treatment with convalescent plasma for influenza A (H5N1) infection. N Engl J Med **2007**; 357:1450–1.
17. Carter PJ. Potent antibody therapeutics by design. Nat Rev Immunol **2006**; 6:343–57.
18. Marasco WA. Sui J. The growth and potential of human antiviral monoclonal antibody therapeutics. Nat Biotechnol **2007**; 25:1421–34.

19. Holliger P. Hudson PJ. Engineered antibody fragments and the rise of single domains. Nat Biotechnol **2005**; 23:1126–36.
20. Greenberg AS. Avila D. Hughes M. Hughes A. McKinney EC. Flajnik MF. A new antigen receptor gene family that undergoes rearrangement and extensive somatic diversification in sharks. Nature **1995**; 374:168–73.
21. Hamers-Casterman C. Atarhouch T. Muyldermans S. et al. Naturally occurring antibodies devoid of light chains. Nature **1993**; 363:446–8.
22. De Genst E. Silence K. Decanniere K. et al. Molecular basis for the preferential cleft recognition by dromedary heavy-chain antibodies. Proc Natl Acad Sci U S A **2006**; 103:4586–91.
23. Baral TN. Magez S. Stijlemans B. et al. Experimental therapy of African trypanosomiasis with a nanobody-conjugated human trypanolytic factor. Nat Med **2006**; 12:580–4.
24. Coppieters K. Dreier T. Silence K. et al. Formatted anti-tumor necrosis factor alpha VHH proteins derived from camelids show superior potency and targeting to inflamed joints in a murine model of collagen-induced arthritis. Arthritis Rheum **2006**; 54:1856–66.
25. Cortez-Retamozo V. Backmann N. Senter PD. et al. Efficient cancer therapy with a nanobody-based conjugate. Cancer Res **2004**; 64:2853–7.
26. De Haard HJ. Bezemer S. Ledeboer AM. et al. Llama antibodies against a lactococcal protein located at the tip of the phage tail prevent phage infection. J Bacteriol **2005**; 187:4531–41.
27. Dumoulin M. Last AM. Desmyter A. et al. A camelid antibody fragment inhibits the formation of amyloid fibrils by human lysozyme. Nature **2003**; 424:783–8.
28. Roovers RC. Laeremans T. Huang L. et al. Efficient inhibition of EGFR signaling and of tumour growth by antagonistic anti-EFGR Nanobodies. Cancer Immunol Immunother **2007**; 56:303–17.
29. Reed LJ. Muench H. A simple method for estimating fifty percent endpoints. Am J Med Hyg **1938**; 27:493–7.
30. Stech J. Stech O. Herwig A. et al. Rapid and reliable universal cloning of influenza A virus genes by target-primed plasmid amplification. Nucleic Acids Res **2008**; 36:e139.
31. Yamada S. Suzuki Y. Suzuki T. et al. Haemagglutinin mutations responsible for the binding of H5N1 influenza A viruses to human-type receptors. Nature **2006**; 444:378–82.
32. Hensley SE. Das SR. Bailey AL. et al. Hemagglutinin receptor binding avidity drives influenza A virus antigenic drift. Science **2009**; 326:734–6.
33. Wiley DC. Wilson IA. Skehel JJ. Structural identification of the antibody-binding sites of Hong Kong influenza haemagglutinin and their involvement in antigenic variation. Nature **1981**; 289:373–8.
34. Perdue ML. Suarez DL. Structural features of the avian influenza virus hemagglutinin that influence virulence. Vet Microbiol **2000**; 74:77–86.
35. Uyeki TM. Human infection with highly pathogenic avian influenza A (H5N1) virus: review of clinical issues. Clin Infect Dis **2009**; 49:279–90.
36. Sun L. Lu X. Li C. et al. Generation, characterization and epitope mapping of two neutralizing and protective human recombinant antibodies against influenza A H5N1 viruses. PLoS One **2009**; 4:e5476.
37. Chen Y. Qin K. Wu WL. et al. Broad cross-protection against H5N1 avian influenza virus infection by means of monoclonal antibodies that map to conserved viral epitopes. J Infect Dis **2009**; 199:49–58.
38. Hanson BJ. Boon AC. Lim AP. Webb A. Ooi EE. Webby RJ. Passive immunoprophylaxis and therapy with humanized monoclonal antibody specific for influenza A H5 hemagglutinin in mice. Respir Res **2006**; 7:126.
39. Maneewatch S. Thanongsaksrikul J. Songserm T. et al. Human single-chain antibodies that neutralize homologous and heterologous strains and clades of influenza A virus subtype H5N1. Antivir Ther **2009**; 14:221–30.
40. Simmons CP. Bernasconi NL. Suguitan AL. et al. Prophylactic and therapeutic efficacy of human monoclonal antibodies against H5N1 influenza. PLoS Med **2007**; 4:e178.
41. Corti D. Suguitan AL Jr. Pinna D. et al. Heterosubtypic neutralizing antibodies are produced by individuals immunized with a seasonal influenza vaccine. J Clin Invest **2010**; 120:1663–73.
42. Ekiert DC. Bhabha G. Elsliger MA. et al. Antibody recognition of a highly conserved influenza virus epitope. Science **2009**; 324:246–51.
43. Kashyap AK. Steel J. Oner AF. et al. Combinatorial antibody libraries from survivors of the Turkish H5N1 avian influenza outbreak reveal virus neutralization strategies. Proc Natl Acad Sci U S A **2008**; 105:5986–1.
44. Okuno Y. Isegawa Y. Sasao F. Ueda S. A common neutralizing epitope conserved between the hemagglutinins of influenza A virus H1 and H2 strains. J Virol **1993**; 67:2552–8.
45. Saerens D. Ghassabeh GH. Muyldermans S. Single-domain antibodies as building blocks for novel therapeutics. Curr Opin Pharmacol **2008**; 8:600–8.
46. Huang L. Gainkam LO. Caveliers V. et al. SPECT imaging with 99mTc-labeled EGFR-specific nanobody for in vivo monitoring of EGFR expression. Mol Imaging Biol **2008**; 10:167–75.
47. Klasse PJ. Sattentau QJ. Mechanisms of virus neutralization by antibody. Curr Top Microbiol and Immunol **2001**; 260:87–108.
48. Wang P. Yang X. Neutralization efficiency is greatly enhanced by bivalent binding of an antibody to epitopes in the V4 region and the membrane-proximal external region within one trimer of human immunodeficiency virus type 1 glycoproteins. J Virol **2010**; 84:7114–23.
49. Suarez DL. Perdue ML. Cox N. et al. Comparisons of highly virulent H5N1 influenza A viruses isolated from humans and chickens from Hong Kong. J Virol **1998**; 72:6678–88.
50. Matrosovich M. Zhou N. Kawaoka Y. Webster R. The surface glycoproteins of H5 influenza viruses isolated from humans, chickens, and wild aquatic birds have distinguishable properties. J Virol **1999**; 73:1146–55.